Novel Cardioprotective Effects of Ferroptosis Inhibitors in Human-Derived Induced Pluripotent Cardiomyocytes in Response to Hypoxic Conditions

Sara Petollari*, Zachary C. Sanchez, Dylan T. Burnette*

Department of Cell and Developmental Biology, Vanderbilt University, Nashville, TN, USA 37203

KEYWORDS. Ferroptosis, Calcium Dynamics, Sarcomere, Hypoxia

BRIEF. Zileuton and Ferrostatin-1s potential to mitigate hypoxia's impact on calcium metabolism and sarcomere structure.

ABSTRACT. Ferroptosis, an iron-dependent form of cell death, has recently been implicated in various cardiovascular diseases. Zileuton and Ferrostatin-1 are FDA approved drugs discovered to exhibit ferroptosis-inhibiting abilities; however, their impact on cell health under hypoxic conditions remains unclear. Here, fluorescence microscopy was used to investigate cytosolic Ca^{2+} dynamics and sarcomere formation, indicators of cell health, in hiCM cardiomyocytes afflicted with Oxyrase-induced hypoxia and receiving drug treatment. The Oxyrase treatment exhibited a significant increase in basal fluorescence and a decrease in the change of fluorescence. Conversely, the Zileuton-Oxyrase treatment significantly reduced Ca^{2+} maximal fluorescence and change in flux. This data suggests that Zileuton minimizes part of hypoxia's effects, likely by inhibiting the 5-lipoxygenease enzyme, responsible for producing leukotrienes which contribute to calcium overload. Ferrostatin-1 treatments exhibited no changes in Ca^{2+} flux, suggesting its lack of beneficial metabolic response and its mitigation of hypoxic effects. Furthermore, sarcomere data portrayed a significant decrease in sarcomere count for Oxyrase and a significant increase in sarcomere precursors for both Oxyrase and Oxyrase-Ferrostatin, whereas Zileuton seemed to prevent this increase. These findings illustrate hypoxia-induced sarcomere damage and suggest a potential therapeutic response facilitated by Ferrostatin-1 and Zileuton. Additionally, they underscore the capacity of Zileuton and Ferrostatin-1 to alleviate hypoxia's detrimental effects on sarcomere structure.

INTRODUCTION.

Cardiovascular diseases (CVD) remain the leading cause of mortality worldwide. In 2020, an estimated 250 million individuals were identified as living with ischemic heart disease, causing 19 million deaths [1]. Notably, myocardial infarctions, or heart attacks, alone contribute to 3.1% of the overall CVD prevalence in the U.S. between 2015 and 2018, causing a substantial mortality rate of 144,050 individuals, as reported in 2019 [1]. Whereas the significant impact of myocardial infractions is well understood societally, preventative measures against them remain lacking.

Ferroptosis, an iron dependent, non-apoptotic cell death characterized by lipid reactive oxygen species (ROS) accumulation [2]. Recent studies implicate ferroptosis as a major driver of CVD. For example, Lip-1, an inhibitor of ferroptosis, protected the heart by reducing myocardial infarct size and maintaining the structural integrity of mitochondria in a mice model looking at ischemia/reperfusion injuries [3].

Numerous drugs like Ferrostatin-1 have been identified as direct inhibitors of ferroptosis. Ferrostatin-1 has demonstrated effectiveness in preventing erastin-induced cytosolic and lipid ROS accumulation in vivo [5]. Additionally, it mimics the anti-ferroptotic effects of Glutathione peroxidase 4, an enzyme responsible for the mitigation of lipid peroxidation during ferroptosis [6]. This further highlights its potential as a therapeutic target for CVDs. Another drug, Zileuton, commonly used to battle asthma, has shown promise as a ferroptosis inhibitor by effectively safeguarding neurons from glutamine-induced oxidative stress resembling the process seen in ferroptosis [7]. Given these promising findings, Zileuton was selected for this study as well. Both Ferrostatin-1 and Zileuton present potential for addressing myocardial infarctions, making them prime candidates for further research.

While these drugs have shown promising results in combatting ferroptosis, their performance under hypoxic conditions, typical in myocardial infractions, remains unclear. This study simulates heart attack conditions in human-derived induced pluripotent stem cell cardiomyocytes (hiCMs) by incubating them in 2% Oxyrase, a reagent that reduces available oxygen in the media. Therefore, the aim is to evaluate Ferrostatin-1 and Zileuton's capability in promoting cardiomyocyte health in hypoxic conditions.

To evaluate cell health, cytoplasmic Ca^{2+} dynamics was analyzed. As a secondary messenger, Ca^{2+} exhibits remarkable versatility, participating in enzyme activities, ion channel regulation, and cell growth. Of particular interest is its involvement in apoptosis and contraction events. In apoptosis, Ca^{2+} primarily impacts processes like endoplasmic reticulum (ER) stress or mitochondrial permeabilization. The former can be caused through the overload or depletion of the ER Ca^{2+} pool, activating the pro-caspase-12 enzyme which then induces apoptosis [8]. The latter can be caused through the excessive mitochondrial uptake of Ca^{2+}, triggering cytochrome c release, activating apoptosis as a result [8]. Furthermore, calcium waves, released by intracellular stores periodically, have been shown to correlate with contraction, relaxation, and excitability control in muscle cells [9]. Understanding these roles of Ca^{2+}, cell health can be evaluated. After ascertaining a baseline and observing changes caused by hypoxic conditions, treatments will be evaluated for their effectiveness. Another chosen metric of cell health was sarcomere structure, crucial to cardiomyocytes' health as their fundamental structural and functional units responsible for contraction events in cardiomyocytes [10]. SarcApp enables high-throughput binarization of raw images and the analysis of multiple sarcomeric features, generating quantitative data on sarcomere structure to analyze impacts on cell structural changes [11].

This research seeks to discover cardioprotective effects of already utilized drug treatments. It involves a novel approach that employs Oxyrase-induced hypoxia to replicate conditions akin to a heart attack. This is a necessary initial step towards future exploration of ferroptosis-inhibiting drugs in the context of myocardial infarction treatment.

MATERIALS AND METHODS.

Cell Culture and Plating.

hiCM cardiomyocytes were cultured as per manufacturer's instructions in proprietary manufacturer-provided cell maintenance medium (CMM) in polystyrene 96-well cell culture plates and maintained at 37 ℃ and 5% CO_2. For re-plating, cells were washed

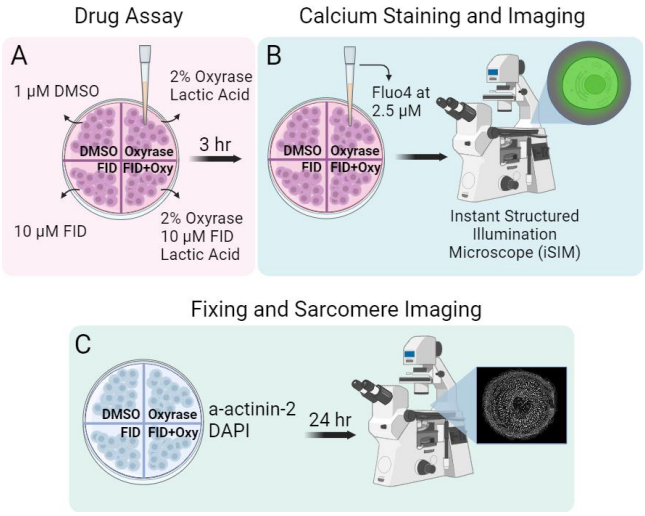

Figure 1. Methodology Overview. A) hiCMs were plated on a 4-well MatTek dish and treated with their respective treatments per well. The cells were then allowed to incubate for a duration of 3 hours. B) Following this incubation period, the culture medium was replaced, and Fluo4 was added to label cytosolic Ca^{2+} fluorescence. Subsequently, the cells were imaged using the iSIM. C) Lastly the cells were fixed and immunostained for a-actinin 2 and stained with DAPI to label the nucleus. FID: Ferroptosis-Inhibiting Drug.

twice with Ca^{2+} /Mg^{2+}-free PBS, treated with 0.1% Trypsin, incubated at 37℃ for 2 minutes, detached through gentle pipette mixing. The trypsin was deactivated with CMM and then the cells were centrifuged at 1000 rpm for 3 minutes. The supernatant was aspirated, and the pellet was re-suspended in CMM and plated on a 35mm 4-well MatTek plate, coated by 10 µg/ml fibronectin. After incubating for 1 hour at 37℃, 300 µL of CMM was added to each well and cells were allowed to grow overnight.

Drug Treatments.

The cells were treated with Zileuton and Ferrostatin-1, previously dissolved in DMSO, at a 10 µM concentration. Hypoxia was induced by adding 2% Oxyrase, which was activated using 20mM Lactic Acid. Previous studies have determined Oxyrase to be an effective O_2 scavenger [12]. After a 3-hour incubation, imaging was performed.

Fluo-4 Cytoplasmic Calcium Staining.

After replacing the media, Fluo-4 was added to each well at a concentration of 2.5 µM. The cells were incubated for 30 minutes before imaging, after which the media was replaced with fresh CMM.

Fixation Process.

The cells were fixed with 4% paraformaldehyde (PFA) at room temperature for 20 minutes. After PFA aspiration, Triton X-100 was added at a 1:100 dilution with 4% PFA per well at room temperature for 5 minutes. Following 3 washes with PBS, the cells were blocked in 5% bovine serum albumin (BSA) in PBS for 20 minutes. α-actinin 2 antibody was added at a 1:200 dilution in BSA to each well after aspiration and left overnight at -4℃. After three washes with BSA, goat anti-mouse alexa fluor 568 was added at a dilution of 1:100 to each well after being centrifuged at 10000 RPM for 2 minutes and left at room temperature for an hour. Following three PBS washes, DAPI was added at 1µg/mL. After 40 minutes at room temperature, the wells were washed three times with PBS and kept in PBS for imaging.

Fluo-4 fluorescence and Sarcomere imaging.

An Instant Structured Illumination Microscope (iSIM) was used with a Nikon SR HP Apo TIRF 60x oil immersion objective and a

Table 1. Key Resources

Designation	Source	Identifier
iCell Cardiomyocytes^2 Kit (hiCMs)	Fujifilm Cell Dynamics	01434
PBSCa^{2+} /Mg2+ free	Life Technologies	70011-044
0.5% Trypsin	Life Technologies	15400-054
Fibronectin	Corning	354008
Fluo4	Invitrogen	F14201
Anti-sarcomeric a-actinin antibody	Abcam	AB9465
Bovine Fraction V (BSA)	RPI	A30075-100.0
DAPI	ThermoFisher	D1306
Triton X-100	ThermoFisher	A16046.AP
Alexa Fluor 568 goat anti-mouse	Invitrogen	A11004
Paraformaldehyde, 16%	Electron Microscophy Sciences	15710
DMSO, Anhydrous	ThermoFisher	D12345
Ferrostatin-1	Sigma-Aldrich	SML0583
Oxyrase	Sigma-Aldrich	SAE0010
Zileuton	Sigma-Aldrich	PHR2555-200MG
Fiji	NIH	
sarcApp	[11]	
yoU-Net	[11]	

Hamamatsu ORCS-Fusion Digital CMOS camera with a 0.2 µm axial step size. Fluo-4 was imaged at 15 laser power and 50ms exposure time for 5 seconds. Sarcomeres, particularly a-actinin-2, were imaged at 40 laser power as z-series with a of 4.6-micron stack size. Subsequently, image deconvolution was performed using Microvolution software in Fiji.

Analysis Programs.

Ca^{2+} flux was analyzed using Fiji and sarcomere structure using sarcApp [12]. Results were visualized with SuperPlots and t-tests were performed using Prism GraphPad. Treatments are compared to DMSO and statistical differences are shown.

RESULTS.

To analyze changes in cardiomyocyte metabolic function, Fluo4, which stains cytosolic Ca^{2+}, was used and imaged for the aforementioned drug treatments for five seconds (Figure 2A&B). When observing basal Ca^{2+} flux, the Oxyrase treatment exhibited a significantly higher amount of fluorescence when compared to the DMSO treatment ($p=0.0016$) (Figure 2C). For the Zileuton-Oxyrase treatment, maximal Ca^{2+} fluorescence was significantly lower when compared to the DMSO treatment ($p<0.0001$) (Figure 2D). Lastly, the Oxyrase and Zileuton-Oxyrase treatments exhibited a significantly lower change in Ca^{2+} flux compared to DMSO ($p<0.0001$) (Figure 2E). The Ferrostatin-1 treatment was the only one to exhibit a significant increase in Ca^{2+} wave count ($p=0.0372$) (Figure 2F).

Additionally, the α-actinin 2 antibody was used to stain sarcomeres for all 6 treatments (Figure 3A). Sarcomere structure was evaluated by analyzing Z-Line and Z-Body structures, proxies for the number of sarcomeres and sarcomere precursors respectively, to evaluate muscle

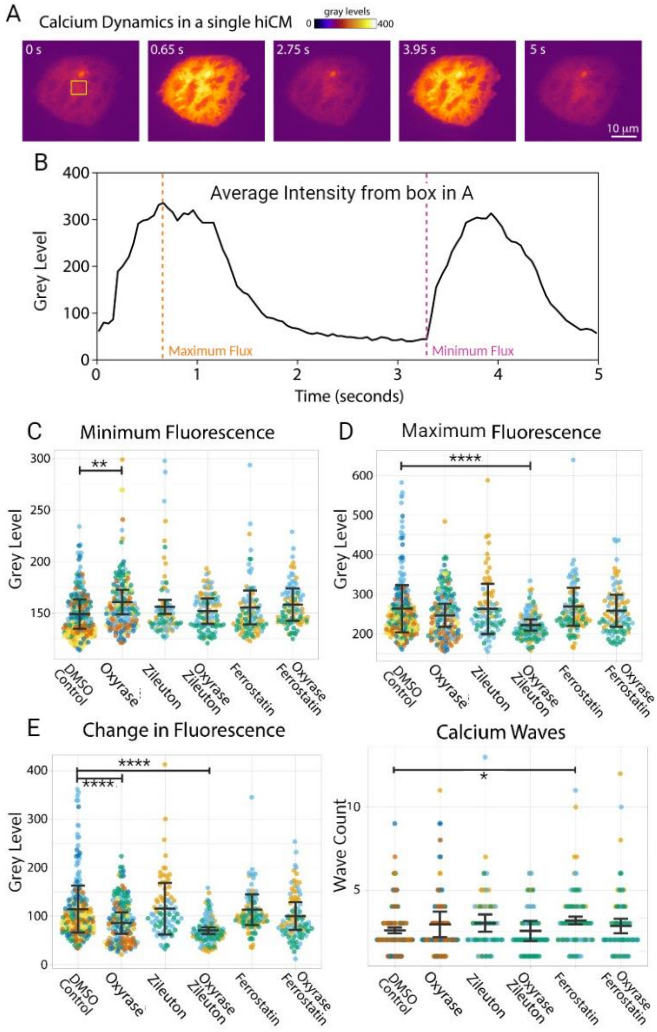

Figure 2: Zileuton Exhibits Cardioprotective Effects through Metabolic Response A) Cytosolic Ca^{2+} fluorescence in a single human induced pluripotent stem cell-derived cardiac myocyte (hiCM) over 5 seconds. B) Average fluorescence intensity from box in Figure 2A with maximum and minimum fluorescence depicted. C) Minimum/Basal average cytosolic Ca^{2+} fluorescence in hiCMs. N=3 biological replicates for all treatments except Oxyrase and DMSO with N=6 replicates. 196 DMSO, 158 Oxyrase, 78 Zileuton, 100 Oxyrase-Zileuton, 90 Ferrostatin-1, and 88 Ferrostatin-Oxyrase cells. D) Maximum average cytosolic Ca^{2+} fluorescence for hiCM in Figure 2C. E) Change in average cytosolic Ca^{2+} fluorescence, as calculated by the difference between maximum and minimum fluorescence, for hiCM in Figure 2C. F) Calcium Wave count for hiCM in Figure 2C. The colors represent different Ns. *p<0.05, **p<0.01, ***p<0.001, ****p<0.0001.

development and cell health. The Oxyrase treatment portrayed a significant decrease in number of Z-Lines compared to the control treatment (p<0.0001) (Figure 3C). As for the Z-Bodies, both Oxyrase and Ferrostatin-Oxyrase exhibited a significant increase compared to DMSO (p<0.0001) (Figure 3B).

DISCUSSION.

The aim of this study was to evaluate the validity of Zileuton and Ferrostatin as therapeutic targets for minimizing the damage caused by myocardial infarctions. To do so, Ca^{2+} flux was quantified in hiCM cardiomyocytes under Oxyrase-induced hypoxia. As previously established, the ER and mitochondria are the organelles most involved in maintaining calcium homeostasis within cells [13,14]. Whereas the

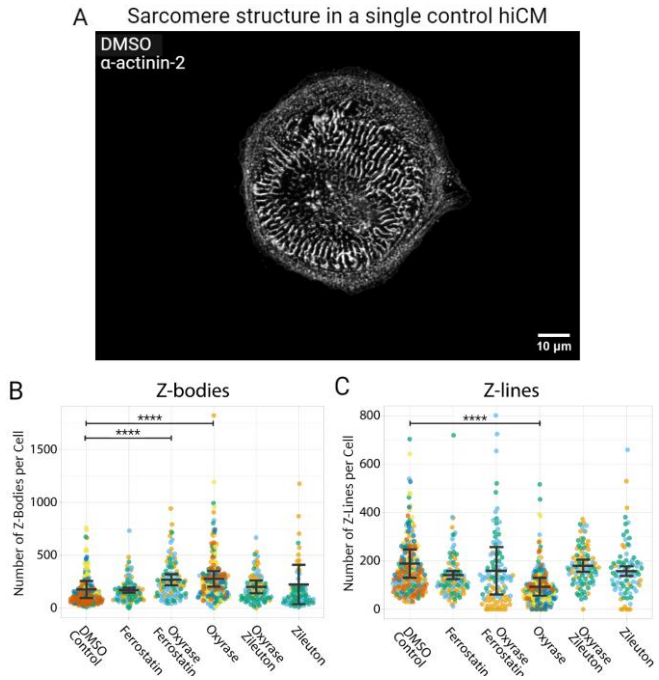

Figure 3: Oxyrase Causes Changes to Sarcomere Structure in hiCMs following 3 hours of exposure. A) Representative image of sarcomeric protein α-actinin-2 in in a single control human induced pluripotent stem cell-derived cardiac myocyte (hiCM). B) Number of Z-Bodies per hiCM cell. N=3 biological replicates for all treatments except Oxyrase and DMSO with N=6 replicates. 202 DMSO, 190 Oxyrase, 79 Zileuton, 90 Zileuton-Oxyrase, 99 Ferrostatin-1, and 104 Ferrostatin-Oxyrase cells. C) Number of Z-Lines for hiCM cells in Figure 3B. The colors represent different Ns.****p<0.0001.

ER functions as the larger Ca^{2+} store, is the site of protein folding, and is responsible for the release of Ca^{2+} to other organelles [13], mitochondria store and uptake Ca^{2+} to produce ATP [14]. Because of this, cytosolic Ca^{2+} levels are likely to change because of these organelles' functions.

Zileuton Assay.

When subjected to Oxyrase treatment, cells displayed a significantly elevated baseline Ca^{2+} fluorescence. This could be attributed to increased ER leakage, reduced mitochondrial Ca^{2+} uptake, or a synergistic combination of both factors. In a hypoxic environment, the ER undergoes significant stress, a state characterized by the accumulation of improperly folded proteins within the ER [15]. This is due to the oxygen-dependent formation of disulfide bonds within the ER during protein folding. Therefore, in an oxygen-deprived environment, the ER may struggle to effectively facilitate protein folding [16]. This misfolding often initiates the Unfolded Protein Response, a mechanism attempting to restore calcium homeostasis in the ER by increasing protein folding capacity and reducing the load of misfolded proteins, causing disruptions in normal cellular function and contribute to the development and progression of various CVDs [17]. However, as part of this response, the ER releases calcium into the cytosol in an attempt to activate signaling pathways to help manage ER stress [17]. Observing an elevated basal fluorescence in cells under Oxyrase-induced hypoxia potentially indicates significant ER stress, a sign of deteriorating cell health. Conversely, hypoxic conditions impede mitochondrial Ca^{2+} uptake by inhibiting cellular respiration [14]. Mitochondria requires ATP to uptake Ca^{2+} and is not successful under hypoxic conditions. Thus, an increased basal Ca^{2+} fluorescence can also be evidence of insufficient supply of ATP.

The data showed that cells under Oxyrase-induced hypoxia treated with Zileuton exhibited a significantly lower level of maximal Ca^{2+} fluorescence. Zileuton is widely known as an inhibitor of the 5-lipoxygenase enzyme (5-LOX), a catalyst that produces leukotrienes (LTs) within cells [7]. Hypoxia has been established as a stimulant for increased LT production, as evidenced by the upregulation of 5-LOX under hypoxic conditions [18]. Previous studies suggest that the decrease in LT production from 5-LOX inhibitors decreased ionized calcium overload as a result of I/R induced arrhythmias [19]. As hypoxia increases LT production and inhibiting LTs reduces calcium overload, the decline in maximal fluorescence in the Zileuton-Oxyrase treatment suggests 5-LOX enzyme inhibition as a likely cause. Consequently, this reduction in maximal fluorescence likely signifies a beneficial response to hypoxic conditions, contributing to cellular health preservation.

Lastly, the significant decrease in Ca^{2+} fluorescence change for both the Zileuton-Oxyrase and Oxyrase treatments must be addressed. The former is explained by the previously mentioned significant maximal fluorescence decrease, while the latter, despite increased basal Ca^{2+} fluorescence, presents a peculiar scenario. This result is likely caused by hypoxia's impact on Ca^{2+} channels that are maintaining homeostasis across the cell and the maintenance of calcium waves in turn. These waves occur when calcium is released by the ER while being shunted out of the cell through Ca^{2+} channels on the plasma membrane. Previously, hypoxia has been implicated to reduce the activity of these channels [21]. This reduction in activity suggests that the increase in basal Ca^{2+} fluorescence would not affect maximal fluorescence, resulting in a notable decrease in the change of Ca^{2+} fluorescence. Despite only growing for 24 hours, the hiCMs have developed these channels, as previous research indicates their presence in neonatal cells [20].

Ferrostatin-1 Assay.

Ferrostatin-1 exhibited distinct responses from the Zileuton treatment regarding cytosolic Ca^{2+}. When compared to DMSO, neither Ferrostatin-1 nor the Ferrostatin-Oxyrase treatments showed significant differences in Ca^{2+} fluorescence. Whereas Zileuton inhibits the 5-LOX enzyme and production of LTs, Ferrostatin-1 is a lipid ROS scavenger [22]. Lipid ROS is generated primarily via non-enzymatic lipid peroxidation and enzymatic lipid peroxidation [23]. The former can be initiated by several lipoxygenase enzymes, including 5-LOX, while the latter results from free radicals, like hydroxyl radicals, abstracting hydrogen from polyunsaturated fatty acids [23]. During ferroptosis, the characteristically observed accumulation of ferrous iron (Fe^{2+}) catalyzes the formation of the free hydroxyl radicals through the Fenton reaction [23]. Therefore, non-enzymatic lipid peroxidation is likely characteristically observed during ferroptosis. Consequently, Ferrostatin-1 is more likely to be effective in countering lipid ROS generated from non-enzymatic lipid peroxidation. This implies that enzymatic lipid ROS could be more prevalent during hypoxia, potentially explaining the observed positive changes in Ca^{2+} dynamics with Zileuton treatment.

The significant increase in calcium waves in the Ferrostatin-treated cells is likely attributed to an unintended or off-target effect. Further research is necessary to comprehensively understand the underlying cause of this phenomenon.

Sarcomere Structure Analysis.

The structures of the cardiomyocytes were assessed with immunostaining to see if hypoxia compromised cell integrity. As mentioned earlier, a significant reduction in Z-line formation was prevalent in the hiCMs treated with Oxyrase. A previous study demonstrated an ongoing deterioration in sarcomere structure, as measured by the ratio of sarcomere area to cell area, when subjecting hiCM cardiomyocytes to 8 hours and 24 hours of hypoxia [24]. The above significant difference was unexpected, considering the short-term exposure to Oxyrase. However, this outcome provides additional evidence of cytoskeleton damage caused by hypoxia. Curiously, the Ferrostatin-Oxyrase and Oxyrase treatments exhibited a significant increase in Z-Body formation. Whereas the heightened Z-Body formation in the Oxyrase-treated group is potentially linked to their inability to develop into Z-Lines or to the deterioration of previously existent Z lines [11]. As evidenced by the significant decrease in Z-line numbers, the Ferrostatin-Oxyrase group did not exhibit a corresponding reduction in Z-line formation. Notably, the Zileuton-treated cells exhibited no adverse effects on sarcomere structure and mitigated the effects of hypoxia, supporting Zileuton being a suitable therapeutic target for future CVD research.

CONCLUSION.

The Cardioprotective Effects of Zileuton and Ferrostatin-1.

This study highlights the differing cardioprotective effects of Zileuton and Ferrostatin-1 in hypoxic conditions. Zileuton exhibited favorable metabolic responses, reducing basal and maximal Ca2+ fluorescence. These responses are likely to diminish the possibility of triggering apoptosis or ferroptosis by limiting the calcium that could stimulate their activation cascades. Ferrostatin-1, while lacking direct metabolic benefits, effectively countered Oxyrase-induced hypoxia's detrimental effects, aligning with the control group's cytosolic calcium response. Furthermore, both Zileuton and Ferrostatin-1 demonstrated their ability to mitigate hypoxia-induced damage to sarcomere structure.

Future Directions and Limitations.

In future studies, cellular damage sites resulting from Oxyrase exposure will be explored. The observed increase in basal Ca^{2+} levels under Oxyrase treatment suggests potential mitochondrial damage or ER leakage. Therefore, Ca^{2+} fluorescence will be examined within the mitochondria and ER using genetically encoded calcium indicators [25]. Furthermore, the use of drugs like Cyclosporin A to assess mitochondria and ER-specific dysfunction in response to hypoxia will be explored [26]. Additionally, the potential efficacy of other drugs related to ferroptosis for their potential therapeutic effects can be investigated [27,28]. These, alongside Zileuton and Ferrostatin-1, can be combined to observe their collective effect. This study faced constraints due to limited experiment time and frequency. It is important to note that this investigation was conducted in vitro, lacking certain variables that might be present in vivo. Additional testing within in vivo models, such as mice, is essential.

REFERENCES.

1.C. W. Tsao, Heart disease and stroke statistics—2022 update: A report from the American Heart Association. *Circulation* **145,** 153-639 (2022).

2.J. Li, Ferroptosis: Past, present and future. *Cell Death & Disease* **11**(2) (2020).

3.Y. Feng, Madungwe, N. B. Liproxstatin-1 protects the mouse myocardium against ischemia/reperfusion injury by decreasing VDAC1 levels and restoring GPX4 levels. *Biochemical and Biophysical Research Communications* **520**, 606–611 (2019).

4.A. M. Fratta Pasini, New insights into the role of ferroptosis in cardiovascular diseases. *Cells*, **12**(6), 867-892 (2023).

5.S. J. Dixon, Ferroptosis: An iron-dependent form of nonapoptotic cell death. *Cell*, **149**(5), 1060–1072, (2012).

6.G. Miotto, Insight into the mechanism of ferroptosis inhibition by ferrostatin-1. *Redox Biology* **28**, 101328, (2020).

7.Y. Liu, The 5-lipoxygenase inhibitor Zileuton confers neuroprotection against glutamate oxidative damage by inhibiting ferroptosis. *Biological & Pharmaceutical Bulletin*, **38**(8), 1234–1239, (2015).

8.S. Orrenius, Regulation of cell death: The calcium–apoptosis link. *Nature Reviews Molecular Cell Biology*, **4**(7), 552–565, (2003).

9.S. Wray, Calcium signaling in smooth muscle. *Handbook of Cell Signaling*, 1009–1025, (2010).
10.C. Crocini, M. Gotthardt, Cardiac sarcomere mechanics in health and disease. *Biophysical Reviews*, **13**(5), 637–652, (2021).
11.Neininger-Castro A. C., Independent regulation of Z-lines and M-lines during sarcomere assembly in cardiac myocytes revealed by the Automatic Image Analysis Software sarcapp. *eLife*, **12**, (2023).
12.J. K. Joseph, A novel method of inducing and assuring total anoxia during in vitro studies of O_2 deprivation injury. *Journal of the American Society of Nephrology*, **1**(5), 837–840, (1990).
13.Carreras-Sureda, A., Calcium signaling at the endoplasmic reticulum: Fine-tuning stress responses. *Cell Calcium*, **70**, 24–31 (2018).
14.L. Contreras, Mitochondria: The calcium connection. Biochimica et Biophysica Acta (BBA) - *Bioenergetics*, **1797**(6–7), 607–618, (2010).
15.D. Lindholm, ER stress and neurodegenerative diseases. *Cell Death & Differentiation*, **13**(3), 385–392, (2006).
16.Y. Shimizu, Oxidative folding: Cellular strategies for dealing with the resultant equimolar production of reactive oxygen species. *Antioxidants & Redox Signaling*, **11**(9), 2317–2331, (2009).
17.M. Corazzari, Endoplasmic reticulum stress, unfolded protein response, and cancer cell fate. *Frontiers in Oncology*, **7**, 78 (2017).
18.C. S. Gonsalves, Hypoxia-mediated expression of 5-lipoxygenase–activating protein involves hif-1α and NF-KB and micrornas 135A and 199A-5p. *The Journal of Immunology*, **184**(7), 3878–3888, (2010).
19.E. Gonca, The effects of Zileuton and montelukast in reperfusion-induced arrhythmias in anesthetized rats. *Current Therapeutic Research*, **75**, 27–32, (2013).
20.W. E. Louch, Calcium signalling in developing cardiomyocytes: Implications for model systems and disease. *The Journal of Physiology*, **593**(5), 1047–1063, (2015).
21.B. Liu, Role of TG2-mediated serca2 serotonylation on hypoxic pulmonary vein remodeling. *Frontiers in Pharmacology*, **10**, 1611-1626 (2020).
22.Y. Baba, Protective effects of the mechanistic target of rapamycin against excess iron and ferroptosis in cardiomyocytes. *American Journal of Physiology-Heart and Circulatory Physiology*, **314**(3), 659-668 (2018).
23.J.-Y. Lee, Lipid metabolism and ferroptosis. *Biology*, **10**(3), 184, (2021).
24.M. Häkli, Human induced pluripotent stem cell-based platform for modeling cardiac ischemia. *Scientific Reports*, **11**(1), 4153-4166 (2021).
25.J. Akerboom, Genetically encoded calcium indicators for multi-color neural activity imaging and combination with optogenetics. Frontiers in *Molecular Neuroscience*, **6**, 1-29 (2013).
26.J. Mishra, Cyclosporin a increases mitochondrial buffering of calcium: An additional mechanism in delaying mitochondrial permeability transition pore opening. *Cells*, **8**(9), 1052, (2019).
27.D. Huang, Steroidal saponin SSPH I induces ferroptosis in HEPG2 cells via regulating iron metabolism. *Medical Oncology*, **40**(5), (2023).
28.G. Hasenfuss, Mechanism of action of the new anti-ischemia Drug Ranolazine. *Clinical Research in Cardiology*, **97**(4), 222–226, (2007).

Sara Petollari is a student at Martin Luther King Jr. Magnet High School in Nashville, TN; she participated in a research internship through the School for Science and Math at Vanderbilt.